Paleolimnological response of Ecuadorian páramo lakes reflect both local and regional influences during the last two millennia

Authors: Melina Luethje[1,2] (mluethje@unomaha.edu; ORCID https://orcid.org/0000-0001-8413-461X), Xavier Benito[3] (xavier.benito@irta.cat;ORCID https://orcid.org/0000-0003-0792-2625), Tobias Schneider [4,5] (tobiaschnei@gmail.com; ORCID http://orcid.org/0000-0002-1593-0273), Pablo V. Mosquera[6,7] (pmosquerav@gmail.com; ORCID http://orcid.org/0000-0002-3974-6489), Paul Baker[8] (pbaker@duke.edu), Sherilyn C. Fritz[1] (sfritz2@unl.edu)

[1]Earth and Atmospheric Sciences, University of Nebraska-Lincoln, Lincoln, NE, USA

[2]Department of Geography & Geology, University of Nebraska at Omaha, Omaha, NE, USA

[3] Marine and Continental Waters Programme, Institute of Agrifood Technology and Research (IRTA), Spain

[4]Department of Geosciences, Morrill Science Center, University of Massachusetts, MA, USA

[5]Oeschger Center for Climate Change Research, University of Bern, Bern, Switzerland

[6]Subgerencia de Gestión Ambiental de la Empresa Pública Municipal de Telecomunicaciones, Agua potable, Alcantarillado y Saneamiento (ETAPA EP), Cuenca, Ecuador

[7]Departament de Biologia Evolutiva, Ecologia i Ciències Ambientals, Universitat de Barcelona, Barcelona, Spain

[8]Division of Earth and Ocean Sciences, Duke University, Durham, NC, USA

Corresponding Author: Melina Luethje

Abstract

Increasing surface air temperatures and human influences (e.g., agriculture, grazing, mining, urbanization, tourism) are altering lakes on the Andean páramo of South America, as illustrated by changes in diatom species composition in sediment cores from the region that span the last ~150 years. Previous studies were limited by their relatively short temporal scales and limited spatial coverage. We analyzed sediment cores from the northern (Laguna Piñan) and southern (Laguna Fondococha) Andean páramos of Ecuador. The deposits span the last two millennia and provide a longer-term perspective on past changes in lake ecological and geochemical dynamics. Both lakes show shifts in dominant diatoms through time. Dominant diatom taxa in Fondococha shifted between two *Aulacoseira* species, and there was a change in the planktic to benthic ratio, a proxy for open-water versus shallow-water habitats. Both changes are interpreted as evidence of fluctuating lake level. The inferred lake-level changes are corroborated by stratigraphic variations in the concentration of Ti, an erosional proxy, indicating changes in clastic input as a function of wetter or drier conditions. Piñan shows a directional shift in the diatom assemblage over the period of the record, from benthic diatoms tolerant of high dissolved organic carbon (DOC), low pH, and low nutrients, to an assemblage characteristic of lower DOC, higher pH, higher nutrients, and higher lake levels. Shifts in Piñan's diatoms are correlated with tephra layers in the sediment, suggesting that local volcanic ash deposition may have altered both the catchment and lake geochemistry. This is supported by relatively higher $\delta^{13}C$ values in organic matter associated with tephra layers, which become more negative up-section. Our data suggest that remote lakes in spatially heterogenous montane regions are sentinels of environmental change, and the records from Piñan and Fondococha provide insights into Andean ecosystem responses to past environmental perturbations.

Key Words: Paleolimnology, Diatoms, Tropical Andes, Ecuador, Lakes, Páramo, Environmental change

Introduction

Tropical Andean páramos are wet alpine grassland and shrub ecosystems that lie above the tree line and below the permanent snow line (~2800-4700 m asl). Páramos extend from 11°N to 8°S latitude and are concentrated in the northern Andes of Venezuela, Colombia, and Ecuador. Despite their small areal extent, they contain exceptionally high levels of biodiversity and endemism, in association with large variations in topography and climate (Sklenář et al. 2014). The páramo landscape consists of many glacially formed valleys and plains, with scattered lakes, temporary ponds, peat bogs, and wetlands (Buytaert et al. 2006). The combination of a cool and humid climate and porous humic soils makes páramos important regulators of the regional hydrologic cycle (Buytaert et al. 2006), and they supply nearly all the water used for drinking, irrigation, and hydroelectricity in many parts of the northern Andes and adjacent Amazon lowlands.

Páramo ecosystems are currently threatened by several ecological stressors. In the Andes, accelerated warming within the last few decades (Vuille and Bradley 2000; Vuille et al. 2003) has resulted in the retreat of glaciers, alteration of the hydrologic cycle, and shifting ranges of plant and animal species (Vuille et al. 2008; Rabatel et al. 2013; Morueta-Holme et al. 2015). Simultaneously, human activities including agriculture, grazing, mining, urban expansion, and tourism have increased (Buytaert et al. 2006). Understanding how these ecosystems respond to climate change and human activities is important for regional conservation planning, climate change adaptation, and water security (Ochoa-Tocachi et al. 2019).

The Ecuadorian Andean páramos contain a high density of lakes (Mosquera et al. 2017) that are ideal ecosystems for evaluating regional environmental change. Paleolimnological studies of Ecuadorian lakes have investigated the ecological and biological responses of such lakes to recent climate-related changes, such as increasing air temperature and decreasing wind speed (Michelutti et al. 2015a; Giles et al. 2017; Frederick et al. 2018). For example, increases in the diatom species *Discostella stelligera* (Cleve and Grunow) Houk and Klee 2004 were associated with changes in lake thermal regime (Michelutti et al. 2015a). Those studies, however, were restricted spatially (mainly southern Ecuador) and investigated only the last century or two and may not be representative of longer-term trends or the broader Ecuadorian páramos. Furthermore, a recent landscape-scale paleolimnological analysis of Ecuadorian lakes

demonstrated that limnological change induced by climatic and/or anthropogenic stressors was not spatially widespread during the last ~150 years, suggesting that diatom communities, and lakes by inference, were ecologically resilient over a broad geographic range and over time scales longer than the last century (Benito et al. 2019).

We investigated the paleolimnology of two páramo lakes located in the north (Laguna Piñan) and south (Laguna Fondococha) of Ecuador (Fig. 1) to infer their ecological responses to external drivers over the last two millennia. We chose two spatially distant, relatively deep (z_{max} >9 m) lakes and used stratigraphic changes in the diatom flora and sediment geochemistry to explore whether the two responded synchronously to past environmental changes. The contemporary diatom flora and the lake physico-chemical variables were sampled to use as a baseline for comparison to paleolimnological changes. We hypothesized that if the lakes showed synchronous stratigraphic changes, then the driver(s) were likely regional, i.e., climatic. Alternatively, if detected paleolimnological changes were asynchronous, either local catchment processes mediated climate influences or the drivers themselves were local (i.e., land use, catchment geochemistry and/or geomorphology).

Site description

Fondococha (S02°45.6', W79°14.16'; 4130 m asl) and Piñan (N00°31.054', W78°26.292'; 3183 m asl) were chosen for their remote locations and limited local human influences. Fondococha (Figs. 1 and 2A) is in Cajas National Park in the southern Ecuadorian Andes. Pleistocene glacial deposits cover the volcanic bedrock, producing organic-rich Andisol and Histosol soils (Harden et al. 2006). The lake has a surface area of 3.4 ha, with a maximum water depth of 9.9 m. The lake is exorheic and polymictic. Piñan (Figs. 1 and 2B) is in the Cotacachi Cayapas Ecological Reserve in the northern Ecuadorian Andes. It is one of ~35 glacially formed lakes in the region. The landscape, bedrock, and soil are like that of Cajas. The lake area is 195 ha, with a maximum water depth of 32.1 m. The lake is exorheic and polymictic.

Climate in both areas is generally wet and humid. Temperature shows little seasonal variation. In Cajas National Park, where Fondococha is located, temperature varies diurnally

between 3 and 6°C, and annual precipitation ranges from 829 to 1343 mm (Michelutti et al. 2015a). In Cotacachi Cayapas Reserve, the location of Piñan, temperature varies diurnally between 4 and 10°C, and the region has an average annual rainfall of 906 mm. Precipitation for the region originates from easterly flow across the Amazon Basin (Kalnay et al. 1996; ETAPA 2016; Schneider et al. 2018). Both areas have two pronounced rainy seasons, from February to May and October to December, related to the seasonal migration of the Intertropical Convergence Zone (ITCZ; Vuille et al. 2000).

Both Cajas National Park and Cotacachi Cayapas Ecological Reserve are protected natural regions of Ecuador. Cotacachi Cayapas Ecological Reserve was established in 1968, and Cajas National Park in 1996. Like other areas of the páramo, humans have influenced these regions for at least hundreds of years (Hansen et al. 2003; Sarmiento 2012). However, since their establishment as protected areas, human practices, such as grazing, have decreased (Bandowe et al. 2018). Today, these areas are attractive tourist destinations for nature treks, sport fishing, and camping. These tourist activities have resulted in changes in vegetation cover, introduction of invasive species, and pollution of waterbodies (Barros et al. 2015; Bandowe et al. 2018; Schneider et al. 2021).

Materials and methods

Field work

Short cores (~1 m long) were retrieved during two field seasons, using a percussion gravity-corer with 6-cm-diameter liners (UWITEC, Austria). The sediment-water interfaces were preserved using wet floral foam. Fondococha was cored in July 2014 (Fig. 2). The core was transported to the Institute of Geography, University of Bern, Switzerland, stored in a dark cold room (4°C), and after a sedimentological description (Schnurrenberger et al. 2003) and measurement of the semi-quantitative elemental composition, sampled contiguously at 1-cm intervals. Piñan was cored in July 2017 (Fig. 2). The core was sliced every 1 cm in the field and transported to the Earth and Atmospheric Sciences Department, University of Nebraska-Lincoln, USA. The core was subsampled for chronology, geochemistry, and diatom analysis. Water samples were taken

30 cm below the water surface during July 2017 from both lakes and sent to the Water Sciences Lab (University of Nebraska-Lincoln) for analysis of cations, anions, and major nutrients (TN, TP).

Samples for analysis of contemporary diatom assemblages were collected to provide reference material on the major taxa and their habitat distribution in the modern lakes. Periphyton samples were collected from both lakes along their margins by scraping rocky substrate with a brush and collecting macrophyte plant matter. In each lake, a surface sediment samples (0-1 cm) was collected from the top of each core in the field to represent planktic habitats.

Laboratory methods

Cations in water samples were measured using Atomic Absorption Spectrophotometry. Anions were measured using Ion Chromatography. Total Kjedahl phosphorus (TP) and nitrogen (TN) were measured using colorimetry following, respectively, acid and alkaline persulfate digestion. Additional modern lake physico-chemical characteristics were obtained from the local water utility company (ETAPA EP) of Cuenca (Ecuador) and Laboratory of Aquatic Biology at Campus Kulak Kortrijk (Belgium). Each sediment core was analyzed for basic sedimentological characteristics, geochemistry, and diatom species abundance and composition.

For diatom analysis, approximately 1 g of wet sediment was weighed and freeze dried. Organic matter was removed with 30% hydrogen peroxide. Samples were rinsed with distilled water and then permanently mounted on slides using Naphrax. At least 300 diatom valves were counted at 1000x on a Zeiss Axioskop light microscope with differential interference contrast. Diatoms were identified to species level using both cosmopolitan and regional (Manguin 1964; Servant-Vildary 1986; Metzeltin and Lange-Bertalot 1998) floras. For each sample, diatoms were grouped based on their habitat preferences: planktic (P, free-floating in littoral zone), tychoplanktic (attached to substrates but able to survive in the plankton), and benthic (B, attached to surfaces, such as macrophytes, sand rocks, mud). The ratio of planktic (P) to benthic

(B) diatoms was calculated as a simple metric of changes in open water to shallow water habitat driven by lake level variation (Wolin and Stone 2010).

For Piñan, measurements of TN, TC, and $\delta^{13}C_{org}$ were made at the Department of Geological Sciences Mass Spectrometry Laboratory, University of Florida, using a Thermo Electron DeltaV Advantage isotope ratio mass spectrometer coupled with a ConFlo II interface linked to a Carlo Erba NA 1500 CNHS Elemental Analyzer (Electronic Supplementary Material [ESM] Fig. S1). All carbon isotope results are expressed in standard delta notation relative to Vienna Pee Dee belemnite (VPDB). Geochemical methods on Fondococha are described in Bandowe et al. (2018) and Schneider et al. (2021). Semi-quantitative elemental composition (here, Ti) was measured at 1-mm resolution using a micro-X-ray fluorescence scanner (µXRF, ITRAX) equipped with a Mo-tube (exposure time: 10 s; voltage: 30 kV, current: 35 mA). In the absence of a direct comparison with the Piñan geochemistry record (i.e., C/N ratios), a Ti time-series is included here as an indicator of detrital input from the catchment (Davies et al. 2015).

Statistical analysis

Statistical analyses were performed using R (R Core Team 2019) and C2 software (Version 1.7.7). Diatom relative abundances (%) were calculated and plotted. Diatom zones were identified through hierarchically constrained cluster analysis (CONISS), using the *coniss* function in the *rioja* package, and evaluated for statistical significance with the broken stick model using the *bstick* function in the *rioja* package (Juggins 2017). Diatom rarefied species richness was calculated using the *rarefy* function in the *vegan* package. A principal component analysis (PCA), using diatom species relative abundance data, was run on each lake core using the *prcomp* function in the base *stats* package (R Core Team 2019). Prior to PCA, the diatom data were Hellinger transformed to accommodate linear assumptions (Legendre and Gallagher 2001). Principal components axes PC1 and PC2 were extracted and subsequently plotted against and correlated to geochemical variables using the *cor.test* function in the base *stats* package (R Core Team 2019).

Age-depth models

Core chronologies were established using ^{210}Pb and radiocarbon dating (^{14}C) techniques. The age-depth model of Fondococha was adapted from previous studies. Details about the ^{210}Pb-chronology (CRS, with missing inventory correction, Tylmann et al. 2014) can be found in Bandowe et al. (2018), and information about the age-depth model is specified in Arcusa et al. (2020) and Schneider et al. (2018). Five radiocarbon dates were included in the Fondococha age model. Instantaneously deposited event layers (e.g., tephra layers, flood layers) were masked (omitted) for the age calculations and reinserted in the combined age-depth model. Core correlation between the Fondococha master core (FON-14-1-A) and the cores used for this research (FON-14-2-1-A) was done by visual identification of distinctive strata in the cores, and projection of the associated ages in FON-14-1-A onto our cores.

The ^{210}Pb analyses for Piñan were completed at the St. Croix Watershed Research Station using alpha spectrometry, and a chronology was modeled using the constant-rate-of-supply (CRS) model (Appleby and Oldfield 1978). The entire inventory of unsupported ^{210}Pb was contained within the top 20 cm. Three ^{14}C ages were determined on plant macrofossil remains and were calibrated with the IntCal13 calibration curve (Reimer et al. 2013). A Bayesian age-depth model was constructed using the *rbacon* R package (Blaauw and Christen 2019). Two tephra layers in Piñan (39-43 cm, 52-55 cm) were identified from smear slides under a light microscope and were masked (omitted) for the age calculation and reinserted in the age-depth model.

Results

Modern lake characteristics

Both lakes have broadly similar limnological characteristics with a few exceptions (Table 1). Fondococha is shallower (z_{max} = 9.9 m) than Piñan (z_{max} = 32.1 m), and its surface water

temperature (11.05 °C) was cooler than Piñan (16.5 °C) at the time of measurement. Fondococha is circum-neutral (pH=7.3), whereas Piñan is slightly alkaline (pH=8.7). Conductivity is low (<100 µS cm^{-1}) in both lakes, and ionic composition is similar, although Ca concentration is higher in Fondococha. Both lakes have relatively low TN values. After laboratory analysis of samples collected in 2017, TP values were compared to those collected by colleagues at ETAPA-EP. Our TP values were inconsistent with ETAPA-EP measurements on multiple samples (Van Colen et al. 2017; Mosquera pers. commun.) and were therefore discarded.

Modern diatoms

Diatoms from periphyton samples taken along the lake margin and the core surface sediment (0-1 cm) were counted from both lakes to characterize the modern diatom communities (Fig. 3). The Fondococha periphyton sample (Fig. 3A) was dominated by *Aulacoseira alpigena* (Grunow) Krammer 1991, *Cavinula pseudoscutiformis* (Hustedt) D.G. Mann and A.J. Stickle 1990, *Psammothidium* cf. *grischunum*, and *Achnanthidium macrocephalum* (Hustedt) Round and Bukhtiyarova 1996. In contrast, the surface sediment (Fig. 3B) was dominated by *Aulacoseira distans* var. *septentrionalis* K.E. Camburn and D.F. Charles 2000 (referred to in this manuscript as *A. distans*), *A. alpigena*, and *Achnanthidium minutissimum* (Kützing) Czarnecki 1994.

The Piñan periphyton sample (Fig 3C) consisted of *A. minutissimum*, *Fragilaria capucina* Desmazières 1830, *Fragilaria gracilis Ø*strup 1910, and *Fragilaria tenera* (W. Smith) Lange-Bertalot 1980. The surface sediment (Fig. 3D) consisted of diverse benthic species, dominated by *Nitzschia* cf. *clandestina* Manguin 1964, *Navicula radiosa* Kützing 1844, *Nitzschia* cf. *oberheimiana* U. Rumrich and Lange-Bertalot, *A. minutissimum*, and *Staurosirella pinnata sensu lato* (Ehrenberg) D.M. Williams and Round 1988. Planktic species in the surface sediment were limited and include *A. alpigena* and *Tabellaria fenestrata* (Lyngbye) Kützing 1844.

Age-depth models

The radiocarbon measurements used in the age-depth models are reported in ESM Table S1. For the Fondococha age-depth model (ESM Fig. S1), the top 9 cm contained unsupported ^{210}Pb, yielding an oldest reliable date of AD 1870 (Bandowe et al., 2018). Mass accumulation rate (MAR) ranged between 0.005 and 0.025 g cm^{-2} yr^{1} and was constant prior to AD 1960; after AD 1960, MAR increased.

For the Piñan age-depth model (ESM Fig. S2), a total of 15 samples contained unsupported ^{210}Pb, yielding an oldest reliable date of AD 1870 at a depth of 16 cm. Since AD 1900, the lake has had a mean linear sedimentation rate of 0.13 cm yr^{-1} and a MAR of 0.009 g cm^{-2} yr^{1}. The low mean sediment accumulation rate and relatively high unsupported ^{210}Pb activities compared to cores from other South American lakes suggests that the dates are reliable. A near-constant average sedimentation rate of ~0.1 cm yr^{-1}, similar to that calculated from the ^{210}Pb data, was recorded in the rbacon model. Below the first tephra (52-55 cm), the mean linear sediment accumulation rate was higher, at ~0.3 cm yr^{-1}.

Fondococha diatom stratigraphy

The subfossil Fondococha diatom assemblage contains a total of 134 diatom species. It is characterized by shifts in dominance between *A. alpigena* and *A. distans*, which are coincident with shifts in the planktic to benthic ratio (P:B ratio) (Fig. 4). The benthos includes the genera *Achnanthidium, Amphora, Brachysira, Caloneis, Craticula, Encyonema, Encyonopsis, Eunotia, Gomphonema, Navicula, Neidium, Nitzschia, Pinnularia, Pseudostaurosira, Sellaphora, Staurosirella, and Tabellaria* (ESM Figs. S3-S6). Four stratigraphic diatom zones (FDZ) were identified.

FDZ-1 (96-83 cm, 649-302 BC)

FDZ-1 is numerically dominated by *A. alpigena*, with variable contributions from *A. distans* and benthic taxa (Fig. 4). The interval 99-89 cm (649-302 BC) has a steady abundance of *A. alpigena*. The relative abundance of *A. distans* reaches >40%. The abundance and diversity of benthic species is low. From 88-83 cm (473-302 BC) *A. alpigena* remains dominant, but the abundance of *A. distans* declines. Secondary components include planktic species *F. capucina sensu lato* and benthic species *A. minutissimum*, *N. cryptotenella*, *N. radiosa*, *Sellaphora disjuncta* (Hustedt) D.G. Mann 1989, and *S. laevissima*. Minor contributions from *Amphora*, *Brachysira*, *Encyonopsis*, *Eunotia*, *Gomphonema*, *Neidium*, *Pinnularia*, and *Staurosirella* make this a very taxonomically diverse zone, as supported by high rarefied species richness.

FDZ-2 (82-51 cm, 265 BC - AD 768)

FDZ-2 is dominated by *A. distans* (>50%), with *A. alpigena* accounting for <40% (Fig. 4). The interval from 82-60 cm (265 BC - AD 371) has high P:B ratios and is dominated by *A. distans*, which accounts for >70% of the total assemblage in most samples. The relative abundance of *A alpigena* is low. Relative abundance and diversity of benthic species is also low, except in samples at 80 cm (188 BC) and 67 cm (AD 135) and. At 80 cm, planktic *F. capucina sensu lato* is present. At 67 cm, planktic *Cyclotella* is present. Relative abundance and the composition of benthic species fluctuates from 59 to 51 cm (AD 398-768). *A. distans* peaks (>70%) at 56 cm (AD 541) and 52 cm (AD 718). These peaks coincide with low relative abundance and diversity of benthic species. In contrast, samples with low abundance (<25%) of *A. distans* are observed at 59-58 cm (AD 398-438) and 54 cm (AD 622). These lows coincide with increases in benthic species.

FDZ-3 (50-15 cm, AD 821-1767)

FDZ-3 (Fig. 4) is dominated by *A. alpigena.* From 33 to 15 cm (AD 1472-1767), *F. capucina sensu lato* increases in abundance. *A. distans* abundance varies, ranging from 1% to 57%.

Extreme lows in *A. distans* occur from 50-42 cm (AD 821-1140) and from 33 to 29 cm (AD 1472-1544). When the relative abundance of *A. distans* is lower, benthic species richness increases and the P:B ratio decreases. Benthic species present include *A. minutissimum, Amphora copulata* (Kützing) Schoeman and R.E.M. Archibald 1986, *Brachysira neoexilis* Lange-Bertalot 1994, *Gomphonema gracile* Ehrenberg 1838, *Navicula cryptotenella* Lange-Bertalot 1985, *N. radiosa, Navicula viridulicalcis* Lange-Bertalot 2000, *N.* cf. *clandestina, N.* cf. *oberheimiana, Sellaphora laevissima* (Kützing) D.G. Mann 1989, and *Sellaphora pupula* (Kützing) Mereschkovsky 1902.

FDZ-4 (14-0 cm, AD 1751-2014)

FDZ-4 (Fig. 4) is dominated by the planktic taxa *A. distans*. Secondary components in the plankton include *A. alpigena* and *F. capucina*. The benthic assemblage has low species diversity and low relative abundance (<10%). One peak in *A. alpigena* occurs at AD 1907, coincident with lower values of *A. distans* and higher values of *A. minutissimum* and other benthic species.

Fondococha diatom principal components analysis (PCA)

The first two principal components account for ~75% of the total variability (PC1 = 64.74%, PC2 = 10.35%; Fig 5A). Samples with positive PC1 scores correlated to higher abundances of *A. distans*, whereas samples with negative PC1 scores correlated to higher abundances of *A. alpigena*. Samples with more positive scores on the PC2 axis have higher abundances of *A. minutissimum*, whereas more negative scores are associated with higher abundances of other benthic species. Samples belonging to diatom zones FDZ-1 to FDZ-4 exhibit overlap on the PCA biplot.

Fondococha geochemistry

More complete Fondococha geochemistry results are presented and interpreted in detail in Schneider et al. 2018. Here, we describe the values of Ti (counts per second, cps), and how they fluctuate throughout the core. In FDZ-1 mean values are relatively low (mean Ti = 516.3 cps), which is followed by an increase in FDZ-2 (mean Ti = 720.7 cps). Values then decrease again in FDZ-3 (mean Ti = 573.2 cps) and remain relatively constant throughout FDZ-4 (mean Ti = 587.5 cps). The elemental concentration of Ti is positively correlated with the P:B ratio (r=0.568, p=0.001, ESM Fig. S7A), with PC1 (r=0.505, p=0.01, ESM Fig. S7B), and with *A. distans* relative abundance (r=0.531, p=0.005, ESM Fig. S7C), and it is negatively correlated with *A. alpigena* relative abundance (r=-0.544, p=0.003, ESM Fig. S7D).

Piñan diatom stratigraphy

The Piñan diatom assemblage contains a total of 144 diatom species and has a highly diverse benthic assemblage, with contributions from planktic species increasing up-section (Fig. 6, ESM Figs. S8-S11). Planktic species account for <10% of the total assemblage and include *A. alpigena*, *F. capucina sensu lato*, and *T. fenestrata*. Tychoplankton include the endemic Andean *Pseudostaurosira santaremensis* (Metzeltin and Lange-Bertalot) E. Morales, L. Grana and N.I. Maidana 2018, and *S. pinnata sensu lato*. Benthic diatoms include members from the genera *Achnanthidium, Brachysira, Encyonema, Encyonopsis, Frustulia, Gomphonema, Kobayasiella, Navicula, Nitzschia, Sellaphora, Stauroneis,* and *Stenopterobia.* The dominant benthic taxa shift through time, and three diatom zones (PDZ) were identified.

PDZ-1 (74-38 cm, AD 506-1203)

PDZ-1 is a predominantly benthic diatom assemblage as indicated by the low P:B ratio (Fig. 6). This zone is interrupted by a layer of tephra at 55-52 cm (AD 1004) and contains an interval devoid of diatoms from 58 to 55 cm (AD 925 to 1004). Below the tephra, from 73 to 58 cm (AD

534 to 925), the assemblage contains higher abundances of *Brachysira* and *Nitzschia,* with lesser amounts of *Frustulia*, *Kobayasiella*, and *Navicula*. At 62 cm (AD 794), rarefied species richness increases from a mean of 34 (73-63 cm, AD 506 to 768) to a mean of 39 (62-58 cm, AD 794 to 898). Above the tephra and coarse sand devoid of diatoms, from 52-38 cm (AD 1004 to 1185), the abundance of *F. capucina sensu lato* (~3%) increases slightly. Benthic diatoms are similar to those below the tephra, with the exception of an increase in *Stauroneis* species. A second layer of tephra is deposited at the top of this zone, from 43 to 39 cm (AD 1185).

PDZ-2 (37-26 cm, AD 1221-1423)

In PDZ-2, the P:B ratio increases, indicating a higher contribution of planktic diatoms. This coincides with an increase in tychoplanktic species (>3%) (Fig. 6). In the benthos, *Nitzschia* is the most dominant taxon. Increases in the abundance of *A. minutissimum, Gomphonema,* and *Navicula* are also observed. Notably, *Frustulia, Kobayasiella*, and *Stauroneis* are drastically reduced or absent. Rarefied species richness gradually increases in this zon,e with a mean of 40.

PDZ-3 (25-0 cm, AD 1442-2017)

PDZ-3 has the highest P:B ratio and rarefied species richness in the record (Fig. 6). Members of the plankton consist mainly of *A. alpigena, F. capucina sensu lato,* and *T. fenestrata* (Fig. 6). *Cyclotella sensu lato* is absent from the core, except for the top 4 cm, and *T. fenestrata* is found in the greatest abundance in the upper ~7 cm. Tychoplanktic species also increase in this zone. The benthic assemblage is dominated by *Nitzschia* and *Navicula*. Other members of the benthos include *Achnanthidium*, *Brachysira, Encyonopsis*, and *Stenopterobia densestriata* (Hustedt) Krammer 1987.

Piñan diatom principal components analysis (PCA)

The first two principal components account for ~47% of the total variability (PC1 = 32.2%, PC2 = 14.9%; Fig. 5B). Samples with more positive PC1 scores correlated with higher abundances of *Brachysira*, *Encyonema, Frustulia, Kobayasiella,* and *Stauroneis*. More negative PC1 scores correlated with higher abundances of *A. minutissimum, N. viridulicalcis, N.* cf. *clandestina, N. oberheimiana, P. santaremensis, S. pinnata,* and *T. fenestrata*. Samples with more positive scores on the PC2 are associated with *N.* sp. 1, and *F. tenera,* while more negative scores are associated with *A. minutissimum, E. krammeroides, N. notha, S. pinnata,* and *T. fenestrata*.

Piñan geochemistry

TN ranges from 0 to 1.18 wt. %N (mean=0.49 wt. %N; Fig. 6). TC ranges from 0.07 to 11.82 wt. %C (mean=5.39 wt. %C; Fig. 6). The C/N atomic ratio ranges from 0.07 to 11.68 (mean=5.33; Fig. 6). Finally, $\delta^{13}C$ ranges from -18.92‰ to -11.93‰ (mean=-16.97‰; Fig. 6). The C/N atomic ratio values from 60 to 53 cm (AD 925-1004) and 43 to 39 cm (AD 1185-1203) are low in comparison to the mean value (Fig. 6). The former coincides with a layer of tephra (55-52 cm), and the latter occurs in association with a second layer of tephra at 43-39 cm. From 56 to 54 cm, $\delta^{13}C$ values are less negative than the mean. $\delta^{13}C$ has less negative values prior to the first tephra layer at 55-52 cm and afterward has more negative values. The C/N ratio is negatively correlated with the PC1 (r=-0.566; p=0.01; ESM Fig. S12A) and PC2 (r=-0.574; p=0.01; ESM Fig. S12B) axes from the diatom PCA. Likewise, the $\delta^{13}C$ values are positively correlated with the PC1 (r=0.707; p <0.001; ESM Fig. S12C) axis.

Discussion

Fondococha paleolimnology

Laguna Fondococha's diatom record contains two distinct conditions that alternate through time. The overlap of CONISS clusters when superimposed on the PCA indicates that diatom community shifts correspond to alternation of species rather than complete turnover, and thus do not suggest a shift to a new community state within the investigated period. The first lake condition has a higher abundance of small *A. distans*, lower species richness, higher P:B ratios, and relatively higher values of Ti. The second consists of a higher abundance of the larger *A. alpigena*, higher species richness, lower P:B ratio, and relatively lower values of Ti. The benthic component of the second assemblage varies, but consistently has high relative abundances of *A. minutissimum, Navicula* spp., *Nitzschia* spp., and *Sellaphora* spp. The correspondence of the higher Ti values and higher P:B ratios with higher abundances of *A. distans*, and lower Ti values and lower P:B ratios with higher abundances of *A. alpigena* suggests that the two species occupy different habitats.

The contemporary diatom data give insight into what the two *Aulacoseira* species indicators may infer. *A. distans* var. *septentrionalis* is distinguished from the nominate variety of *A. distans* by its smaller valve size (Genkal et al. 2009). In Fondococha, *A. distans* valve diameter is <6 µm, whereas valve diameters of *A. alpigena* reached >15 µm (ESM Fig. S3). *A. distans* var. *septentrionalis* is a rare taxon that has mainly been reported in the Northern Hemisphere in acidic, low-nutrient, and low-conductivity lakes (Kocioleck 2005; Kharitonov and Genkal 2010). *A. alpigena* is often found living contemporaneously with *A. distans* var. *septentrionalis*, also characteristic of slightly acidic, low-nutrient, and low-conductivity conditions (Kocioleck 2005; Kharitonov and Genkal 2010). In the Andes, both taxa are distributed in Ecuador and Peru and are associated with low conductivity (Fritz et al. 2019). In Fondococha, only valves of *A. alpigena* were observed in a contemporary periphyton sample, whereas both diatoms are observed in the surface sediment collected from the deepest part of the lake, with *A. distans* being the more abundant species (Fig. 3). *A. alpigena* was found in the Quelccaya ice cap, likely originating from wetland pools near the ice cap base, which further suggests it prefers shallow water (Fritz et al. 2015). The distribution of *A. alpigena* in lakes of Ecuador is restricted to shallow páramo lakes (<13 m). In addition to Fondococha, *A. distans* was found in surface sediment of Cajas National Park Lake Dos Chorreras (z_{max}=18 m) (Benito et al. 2019). The contemporary data support that these two species prefer different habitats, with *A. alpigena* in shallower lake areas, and *A. distans* in the deeper central portion of the lake.

Other factors may be responsible for shifts between *A. alpigena* and *A. distans*. For instance, two morphotypes of *A. granulata* found in Spanish reservoirs were differentiated based on light and turbulence (Gómez et al. 1994). Growth strategies in response to nutrient availability could also be influencing the relative abundance of *A. alpigena*. In a study on *Aulacoseira* valves from Finnish lakes of different trophic states, *A. alpigena* was negatively correlated with TP (Turkia and Lepistö 1999). In contrast, in Cajas National Park lakes, TP is higher in shallow lakes (Mosquera pers. commun.), where *A. alpigena* is more abundant. Likely, these shifts between *Aulacoseira* species may be induced by a combination of factors (e.g., nutrient availability, light availability) influenced by lake depth.

Diatom valve size and morphology can affect sinking rates, grazing vulnerability, and nutrient uptake (Rühland et al. 2015). Thus, a reduction in the shallow-water zone would limit the relative abundance of *A. alpigena*, which because of its larger valve size requires greater strength of mixing to remain in the water column. Fondococha has a modern maximum depth of ~10 m (Fig. 2), and its morphometry suggests that under modern or higher lake level, the abundance of planktic diatoms would increase as the area of open water habitat increases (Stone and Fritz 2004). Thus, we interpret times of higher relative abundance of *A. distans* and lower species richness as periods of higher lake level. As lake level decreases, benthic habitat expands and encroaches on the center of the lake, causing greater relative deposition of benthic species. Thus, we interpret higher abundance of *A. alpigena*, higher benthic abundance, and higher species richness as indicating lower lake level.

The geochemistry adds additional support to this interpretation. Ti is commonly used as indicator of detrital input into the lake from the lake catchment (Davies et al. 2015). Higher concentrations may result from increased erosion and catchment runoff as a result of generally wetter conditions or extreme precipitation events (Davies et al. 2015). The overall positive correlation of higher Ti values and *A. distans*, and the strong negative correlations between concentrations of these elements and *A. alpigena* suggests that lake level fluctuations were induced by wet/dry climate phases.

Fluctuations between *A. alpigena* and *A. distans* suggest that lake level varied over the last >2500 calendar years. In FDZ-1, lake level was relatively lower than modern, as inferred from increases in benthic species and low Ti values. Low lake levels were found between 88 and

83 cm (473 to 302 BC). FDZ-2 represents higher lake levels, as inferred from the P:B ratio and the monospecific dominance of *A. distans*. The sedimentology indicates that paleo-flood events increased from ~AD 1020 to 950 (Schneider et al. 2018), and this is further supported by higher values of Ti. We suggest that increased precipitation led to increased lake levels in this interval. FDZ-3 is dominated by *A. alpigena*, representing a period of lower lake level. Decreases in the P:B ratio and subsequent decreases in the values of Ti from 50-42 cm (AD 821 to 1140) and 33-29 cm (AD 1472 to 1544) indicate the shallowest lake levels. FDZ-4 (AD 1767 to 2014) consists of a diatom assemblage similar to modern, with sufficient planktic habitat to support populations of *A. distans*.

Piñan paleolimnology

Laguna Piñan's diatom record exhibits a gradual increase in planktic species through time as indicated by the P:B ratio and the differentiation of benthic and tychoplanktic-dominated CONISS clusters along the PC1 axis. Benthic species in the lake shift after tephra deposition, coincident with shifts in the C/N ratio and $\delta^{13}C_{org.}$ Throughout the core, C/N values fluctuate around a mean value of 5.33, suggesting that the majority of sediment organic matter is autochthonous and associated with algal productivity (Meyers and Teranes 2001). Associated fluctuations in $\delta^{13}C_{org}$ are relatively small. Typical $\delta^{13}C_{org}$ values for lacustrine algae range from -20‰ to -30‰ (Meyers and Teranes 2001); our values are higher (>-19.2‰, Fig. 6), which suggests a significant, but varying macrophyte contribution (Cross et al. 2000). The small decrease in $\delta^{13}C_{org}$ values up-section may indicate an increased contribution of planktic algae in relation to the macrobenthos, corresponding to an increase in the P:B ratio.

PDZ-1 has a relatively high abundance of *Brachysira, Frustulia,* and *Kobayasiella*, which are commonly found in acidic (pH = 5-6), low-nutrient, high dissolved organic carbon (DOC), and low-conductivity lake waters (De Nicola 2000; Wolfe and Kling 2001; Küttim et al. 2017). PDZ-1 is separated by an interval devoid of diatoms from 58-55 cm (AD 925 to 1004), which is adjacent to a tephra layer at 55-52 cm (AD 1004). Above the tephra, higher percentages of *Navicula* and *Stauroneis* species occur. Simultaneously, the $\delta^{13}C_{org}$ becomes more negative and

498 remains low to the present day. This shift could be associated with a small increase in the input
499 of pelagic carbon, perhaps associated with increased water clarity and lower DOC.

500 The interface between PDZ-1 to PDZ-2 is marked by another tephra layer at 43-39 cm
501 (AD 1185). PDZ-2 transitions from an acidic to a circum-neutral/alkaline diatom assemblage, as
502 indicated by the enhanced presence of *N. viridulicalcis*, which has been found in higher pH
503 waters (pH>8; Bahls et al. 2018). The P:B ratio indicates an increase in planktic species.
504 Tychoplanktic species also increase in abundance along with *Nitzschia* spp., including *N.* cf.
505 *clandestina* and *N.* cf. *oberheimiana*. Increases in abundance of *Nitzschia* spp. were also
506 observed in shallow lakes Apicocha and Estrellascocha in Cajas National Park (Giles et al.
507 2018), possibly linked to grazing and burning of the páramo landscape, suggesting increases in
508 lake nutrients. Thus, PDZ-2 marks the beginning of a gradual increase in lake level, as inferred
509 from higher abundance of plankton, and a potential shift towards higher nutrient concentrations.

510 PDZ-3 consists of a higher abundance of nutrient-tolerant, planktic *F. capucina sensu*
511 *lato* and tychoplanktic *Pseudostaurosira* and *Staurosirella* species. Increases in planktic and
512 tychoplanktic taxa likely reflect an increase in planktic habitat resulting from a gradual increase
513 in lake level, or alternatively, draining of surrounding wetland areas. This is supported by an
514 increase in the P:B ratio and a decrease in $\delta^{13}C_{org}$ values up-section, indicating a reduction in
515 macrophyte habitat and an increase in planktic algal productivity.

516 From 9 to 0 cm (AD 1916 to 2017), *T. fenestrata* becomes increasingly abundant. In the
517 Northern Hemisphere, both *F. capucina* and *T. fenestrata* have been found in the plankton of
518 circum-neutral, mesotrophic to eutrophic waters and are indicators of moderate nutrient
519 concentrations (Lowe 1974; Pappas 2010). The coincident depletion in $\delta^{13}C_{org}$ is consistent with
520 an interpretation of higher lake levels and a rise in algal productivity. The increase in the C/N
521 ratio suggests higher inputs from terrestrial organic matter. The village in Piñan has been
522 occupied for ~100 years, which may have resulted in the relative increase in nutrient-tolerant
523 species along the lake margins, because of land-use changes or other anthropogenic influences.
524 One possible explanation is drainage of nearby wetlands, which would alter the lake catchment
525 vegetation and geochemistry, affecting nutrient and macrophyte inputs. Our results point to long-
526 term páramo landscape alterations by humans and lake responses to these processes, even in
527 these remote lake-catchment systems (Sarmiento 2012).

Interpretations between the Piñan core and the Fondococha core are mildly complicated by the littoral coring location of Piñan. Cores taken from the littoral shallow margin of lakes may be more sensitive to factors independent of climate such as macrophyte colonization or erosional inputs from human land-use changes as observed. Further, within the littoral zone, benthic invertebrates have potential to rework the sediment influencing the taphonomy, specifically time averaging, of samples. Despite these issues, the increase in planktic and tychoplanktic species increases towards present indicative of lake level rise. Presumably, if the margin can record this signal, it would be able to record a signal related to climatically induced lake level changes.

Regional comparison

Centennial- to millennial-scale records of climatic change are sparse in South America. Millennial archives spanning the middle to late Holocene document increasing precipitation in several regions of South America, associated with changes in the South American Summer Monsoon (SASM; Tapia et al. 2003; Ekdahl et al. 2008; Vélez et al. 2005; Bird et al. 2011; Cardozo et al. 2014). Centennial variability in moisture and temperature is superimposed on this middle to late Holocene trend (Villota et al. 2017; Frederick et al. 2018; Schneider et al. 2018).

Laguna Pumacocha in the central Peruvian Andes (Fig. 1) has an annually resolved record of $\delta^{18}O_{precip}$ that spans the last ~2 ka and reflects intensification or weakening of the SASM (Bird et al. 2011). Higher $\delta^{18}O$ values from AD 900 to 1000 coincide with the Medieval Climate Anomaly (MCA) and a weaker SASM, whereas lower $\delta^{18}O$ values from AD 1400 to 1820 coincide with the Little Ice Age (LIA) and wetter conditions (Bird et al. 2011). Similar trends are evident in the diatom record from Lake Titicaca (Weide et al. 2017) and in regional speleothem records (Deininger et al. 2019).

Multiple paleolimnological records from the Colombian, Ecuadorian, and Peruvian Andes suggest warmer and/or drier conditions during parts of the MCA (Luning et al. 2019). These include pollen records from Laguna Pindo, Guandera Peat Bog, and Lagunas de Mojanda (Fig. 1), which show upward movement of the tree line from ~AD 500 to 1600 (Giraldo-Giraldo et al. 2018; Moscol Olivera and Hooghiemstra 2010; Velásquez-Ruiz and Hooghiemstra 2013;

Villota et al. 2017). Geochemical records also suggest retreat of glaciers during that time, resulting from warmer and/or drier conditions (Stansell et al. 2013). Our data from Fondococha suggest that the lake was shallower throughout the MCA (AD 900 to 1100) and for several centuries longer, including its shallowest phases between ~AD 1350 and 1500. This was followed by a shift to a deeper lake assemblage in the latter part of the LIA interval, after AD 1750, which persisted until present.

Overall, shifts in the Piñan diatom flora are more unidirectional than those in Fondococha. From AD 506 to 1029, Piñan's diatom assemblage is typical of a shallower, acidic, low-nutrient lake with moderate to high DOC. After that period (AD 1029 to 2017), the dominant diatom species suggest deeper conditions with higher pH, higher nutrients, and lower DOC. These changes coincided with decreases in $\delta^{13}C_{org}$, indicating an increase in algal input to the sediment. The change in the diatom flora could be a function of drier conditions and reduced humic input, but the unidirectional shift in the diatom assemblage regarding lake level, organic matter content, and pH is inconsistent with other regional climate reconstructions (see above) and the lake level changes observed in Fondococha. For example, in nearby Lagunas de Mojanda (Fig. 1), changes in vegetation suggest relatively warmer conditions from ~AD 500 to 1350 and cooler conditions before and after (Villota et al. 2017). This suggests that regional climate had limited influence on the limnology of Piñan, and the influence of local factors appear to have predominated. Piñan's sediment core was taken closer to the lake margin than Fondococha's (Fig. 2), where evidence of local watershed influence may be more pronounced than in deeper lake environments.

The correlation between diatom assemblage shifts and tephra layers offers a secondary explanation for the changes in the Piñan diatom flora. Local ash deposition may have caused a change in soil chemistry and even terrestrial vegetation, which would have altered the ion content, as well as nutrient and organic matter concentrations of the surface and subsurface inflow to the lake (Michelutti et al. 2015b). That, in turn, would have altered lake water chemistry and the composition of the diatom assemblage. Shifts in diatom composition, associated with tephra deposition, were documented previously in Andean lakes (Cruces et al. 2006; Michelutti et al. 2015b).

Increases in diatoms characteristic of planktic and mesotrophic conditions (*F. capucina, T. fenestrata*) within the last ~100 years coincide with the permanent settlement of the nearby village of Piñan. Grazing practices have been documented in the area for >200 years. Grazing of local vegetation could alter the lake catchment and affect runoff to the lake, as found in other lakes in the Ecuadorian Andes. For example, planktic *Fragilaria* species typical of mesotrophic to eutrophic conditions also increased in the top 10 cm of sediment in nearby Huarmicocha (Fig. 1), which was interpreted as reflecting a period of human disturbance near the site (Reidinger 1993). Similarly, in Amazonian Lake Sauce (Fig. 1), increases in *Nitzschia* and *Ulnaria* (an ecologically similar species to *Fragilaria*) corresponded with increased lake nutrients that resulted from agriculture (Bush et al. 2016). This suggests recent human impacts have altered local landscapes and hence the diatom flora.

In contrast to widespread evidence of regional precipitation variation throughout the Andes during the MCA and LIA, with consequent impacts on lake ecosystems, as described above, our data suggest that diatoms in Fondococha and Piñan did not respond simultaneously to climatic influences. Fondococha, the southernmost site, contains a record of fluctuating lake level, likely a regional signal of weakening and strengthening of the SASM. In contrast, Piñan apparently responded most strongly to local catchment changes, possibly related to volcanic tephra deposition, and more recently, to increasing anthropogenic influence. Neither of our records show evidence of pre-Columbian human impacts on the lakes, in contrast to some forested locations in the Andes, where forest clearance and cultivation occurred (Matthews-Bird et al. 2017).

Interpretations of these paleo-records would be strengthened by additional modern studies on diatom ecological and habitat preferences, which are sparse. For example, the Fondococha interpretation would be strengthened by understanding the underlying cause of shifts between the dominant *Aulacoseira* species. Also, spatial factors associated with lake connectivity and landscape position should be considered when studying both modern and paleolimnological diatom assemblages (Anderson 2014; Benito et al. 2018). Further research on the modern limnology of high-mountain tropical lakes may provide additional insights into the differential sensitivity of lakes to changes in surface temperatures, wind speed and direction, precipitation, and vegetation with respect to the lake sediment record.

Acknowledgements

Field work, diatom analysis, Piñan radiocarbon, ^{210}Pb, and geochemical analyses were funded through the National Science Foundation (EAR-1338694), National Geographic Society (8672-09), and a Geological Society of America Graduate Research Grant awarded to Sherilyn C. Fritz (NSF, NGS) and Melina Luethje (GSA). Funding for Fondococha core analysis was obtained through the Swiss National Science Foundation (grant 200021 152986). Tobias Schneider was supported by SNSF early Postdoctoral Mobility Fellowship # P2BEP2_184428. Xavier Benito was supported by the National Socio-Environmental Synthesis Center (SESYNC) under funding received from National Science Foundation DBI-1639145, and the postdoctoral fellowship programme Beatriu de Pinós, funded by the Secretary of Universities and Research (Government of Catalonia) and by the Horizon 2020 programme of research and innovation of the European Union under the Marie Sklodoska-Curie grant agreement No 801370. We thank Jason Curtis for geochemical analyses of the Piñan sediments, and Dan Engstrom for analysis of ^{210}Pb and generation of the age-depth model for the Piñan core. Finally, we are very grateful to Karen Portilla for sharing bathymetric maps and water column data from Piñan.

References

Anderson NJ (2014) Landscape disturbance and lake response: temporal and spatial perspectives. Freshw Rev 7:77–120 doi: 10.1608/FRJ-7.2.811

Appleby PG, Oldfield F (1978) The calculation of lead-210 dates assuming a constant rate of supply for unsupported 210Pb to the sediment. CATENA 5: 1-8 doi: 10.1016/SO341-8162(78)8002-2

Arcusa SH, Schneider T, Mosquera PV, Vogel H, Kaufman D, Szidat S, Grosjean M (2020) Late Holocene tephrostratigraphy from Cajas National Park, southern Ecuador. Andean Geol 47: 508-528 doi: 10.5027/andgeoV47n3-3301

Bahls L, Boynton B, Johnston B (2018) Atlas of diatoms (Bacillariophyta) from diverse habitats in remote regions of western Canada. PhytoKeys 105: 1-186 doi: 10.3897/phytokeys.105.23806

Bandowe BAM, Fränkl L, Grosjean M, Tylmann W, Mosquera PV, Hampel H, Schneider T (2018) A 150-year record of polycyclic aromatic compound (PAC) deposition from high Andean Cajas National Park, southern Ecuador. Sci Total Environ 621: 1652-1663 doi: 10.1016/j.scitotenv.2017.10.060

Barros A, Monz C, Pickering C (2015) Is tourism damaging ecosystems in the Andes? Current knowledge and an agenda for future research. Ambio 44: 82-98 doi: 10.1007/s13280-014-0550-7

Benito X, Fritz SC, Steinitz-Kannan M, et al (2018) Lake regionalization and diatom metacommunity structuring in tropical South America. Ecol Evol 8:7865–7878 doi: 10.1002/ece3.4035

Benito X, Feitl M, Fritz SC, Mosquera PV, Schneider T, Hampel H, Quevedo L, Steinitz-Kannan M (2019) Identifying temporal and spatial patterns of diatom community change in the tropical Andes over the last c. 150 years. J Biogeogr 46: 1889-1900 doi: 10.1111/jbi.13561

Bird BW, Abbot MB, Vuille M, Rodbell DT, Stansell ND, Rosenmeier MF (2011) A 2,300-year-long annually resolved record of the South American summer monsoon from the Peruvian Andes. PNAS 108: 8583-8588 doi: 10.1073/pnas.1003719108

Blaauw M, Christen JA (2019) rbacon: Age-Depth Modelling using Bayesian Statistics. R package version 2.3.6. https://CRAN.R-project.org/package=rbacon doi: 10.1214/11-BA618

Brunschön C, Haberzettl T, Behling H (2010) High-resolution studies on vegetation succession, hydrological variations, anthropogenic impact and genesis of a subrecent lake in southern Ecuador. Veg Hist Archaeobot 19: 191-206 doi: 10.1007/s00334-010-0236-4

Bush MB, Correa-Metrio A, McMichael CH, Sully S, Shadik CR, Valencia BG, Guilderson T, Steinitz-Kannan M, Overpeck JT (2016) A 6900-year history of landscape modification by humans in lowland Amazonia. Quat. Sci. Rev. 141: 52-64 doi: 10.1016/j.quascirev.2016.03.022

Buytaert W, Céleri R, De Biévre B, Cisneros F, Wyseure G, Deckers J, Hofstede R (2006) Human impact on the hydrology of the Andean páramos. Earth-Sci Rev 79: 53-72 doi: 10.1016/j.earscirev.2006.06.002

Cardozo AYV, Gerreira Gomes D, Mendes da Silva E, Duque SRE, Rangel JOC, Sifeddine A, Turcq B, Spadano Albuguerque AL (2014) Holocene paleolimnological reconstruction of a high altitude Colombian tropical lake. Palaeogeogr Palaeoclimatol Palaeoecol 415:127-136 doi: 10.1016/j.palaeo.2014.03.013

Cross S, Baker PA, Seltzer GO, Fritz SC, Dunbar R (2000) A new estimate of the Holocene low stand level of Lake Titicaca and its implications for regional paleohydrology. The Holocene 10: 21-32 doi: 10.1191/095968300671452546

Cruces, F, Urrutia, R, Parra, O, Araneda, A, Treutler, H, Bertrand, S, Fagel, N, Torres, L, Barra, R, Chirinos, L (2006) Changes in diatom assemblages in an Andean lake in response to a recent volcanic event. Arch Hydrobiol 165(1): 23-35 doi:10.1127/0003-9136/2006/0165-0023

Davies SJ, Lamb HF, Roberts SJ (2015) Micro-XRF core scanning in palaeolimnology: Recent developments. In: Croudace IW, Rothwell RG (eds) Micro-XRF Studies of Sediment Cores, Developments in Paleoenvironmental Research. Springer, Dordrecht, pp 189-226 doi: 10.1007/978-94-017-9849-5_7

Deininger M, Ward BM, Novello VF, Cruz FW (2019) Late Quaternary variations in the South American Monsoon System as inferred by speleothems: new perspectives using the SISAL database. Quaternary 2(1): 6 doi: 10.3390/quat2010006

DeNicola DM (2000) A review of diatoms found in highly acidic environments. Hydrobiol 433: 111-122 doi: 10.1023/A:1004066620172

ETAPA (2016) Zonas de vida dentro del Parque Nacional Cajas [URL]. Retrieved from. http://www.etapa.net.ec/Parque-Nacional-Cajas/Biofisico-cultural/Ecologial-Vegetal.

Frederick L, Brunelle A, Morrison M, Crespo P, Johnson W (2018) Reconstruction of the mid Holocene paleoclimate of the Ecuadorian Andean páramo at Tres Lagunas, Ecuador. Holocene 28: 1131-1140 doi: 10.1177/0959683618761547

Genkal SI, Kulikovskiy MS, Dodofeyuk NI (2009) The Centrophyceae from the Nur sphagnous bog (Mongolia). Bot Zhurn 94: 1700-1705

Giles MP, Michelutti N, Grooms C, Smol JP (2018) Long-term limnological changes in the Ecuadorian páramo: Comparing the ecological responses to climate warming of shallow waterbodies versus deep lakes. Freshw Biol 63: 1-10 doi:10.1111/fwb.13159

Giraldo-Giraldo, MJ, Velásquez-Ruiz, CA, Pardo-Trujillo, A (2018) Late-Holocene pollen-based paleoenvironmental reconstruction of the El Triunfo wetland, los Nevados National Park (central Cordillera of Colombia). Holocene 28: 183-194 doi: 10.1177/0959683617721330

Gómez, N, Riera, JL, Sabater, S (1994) Ecology and morphological variability of *Aulacoseira granulata* (Bacillariophyceae) in Spanish Reservoirs. J Plankton Res 17: 1-16 doi: 10.1093/plankt/17.1.1

Hansen BCS, Rodbell DT, Seltzer GO, León B, Young KR, Abbott M (2003) Late-glacial and Holocene vegetational history from two sites in the western Cordillera of southwestern Ecuador. Palaeogeogr Palaeoclimatol Palaeoecol 194: 9-108 doi: 10.1016/S0031-0182(03)00272-4

Harden CP, Hartsig J, Farley KA, Lee J, Bremer LL (2013) Effects of land-use change on water in Andean páramo grassland soils. Ann Am Association Geog 103: 375-384 doi: 10.1080/00045608.2013.754655

Jantz N, Behling H (2011) A Holocene environmental record reflecting vegetation, climate, and fire variability at the Páramo of Quimsacocha, southwestern Ecuadorian Andes. Veg Hist Archaeobot 21: 169-185 doi: 10.1007/s00334-011-0327-x

Kalnay E, Kanamitsu M, Kistler R, Collins W, Deaven D, Gandin L, Iredell M, Saha S, White G, Woollen J, Zhu Y, Chelliah M, Ebisuzaki W, Higgins W, Jaowiak J, Mo KC, Ropelewski C, Wang J, Leetmaa A, Reynolds R, Jenne R, Joseph D (1996) The NCEP/NCAR 40-year reanalysis project. Bull Am Meteorol Soc 77: 437-471 doi: 10.1175/1520-0477*1996)077<0437:TNYRP>2.0.CO;2

Kharitonov VG, Genkal SI (2010) Centric diatom algae (Centrophyceae) of ultraoligotrophic Lake El'gygytgyn and water bodies of its basin (Chukotka, Russia). Inland Water Biol 3: 1-10 doi: 10.1134/S1995082910010013

Kocioleck JP (2005) A checklist of preliminary bibliography of the Recent, freshwater diatoms of inland environments of the continental United States. Proc Calif Acad Sci, 4th Series 56: 395-525

Küttim L, Küttim M, Puusepp L, Sugita S (2017) The effects of ecotope, microtography, and environmental variables on diatom assemblages in hemiboreal bogs in Northern Europe. Hydrobiol 792: 127-149 doi: 10.1007/s10750-016-3050-x

Labaj AL, Michelutti N, Smol JP (2018) Annual stratification patterns in tropical mountain lakes reflect altered thermal regimes in response to climate change. Fund Appl Limnol 191: 267-275 doi: 10.1127/fal/2018/1151

Levkov Z, Blanco S, Krstic S, Nakov T, Ector L (2007) Ecology of benthic diatoms from Lake Macro Prespa (Macedonia). Algol Stud 124: 71-83 doi: 10.1127/1864-1318/2007/0124-0071

Lowe R (1974) Environmental requirements and pollution tolerance of freshwater diatoms. United States Environmental Protection Agency, National Environmental Research Center, Office of Research and Development, Cincinnati, Ohio. EPA-670/4-74-005

Lüning S, Galka M, Bamonte FP, García Rodríguez F, Vahrenholt F (2019) The Medieval Climate Anomaly in South America. Quat Int 508: 70-87 doi: 10.1016/j.quaint.2018.10.041

Manguin E (1964) Contribution á la connaissance des diatomées des Andes du Pérou. Mémoires du Muséum national d'Histoire naturell, Sér B – Botanique 12:41-98

Matthews-Bird F, Brooks SJ, Gosling WD, Gulliver P, Mothes P, Montoya E (2017) Aquatic community response to volcanic eruptions on the Andean flank: evidence from the palaeoecological record. J Paleolimnol 58: 437-453 doi: 10.1007/s10933-017-0001-0

Matthews-Bird F, Valencia BG, Church W, Peterson LC, & Bush M (2017). A 2000-year history of disturbance and recovery at a sacred site in Peru's northeastern cloud forest. Holocene 27: 1707-1719

Metzeltin D, Lange-Bertalot H (1998) Tropical diatoms of South America I. Iconographia Diatomologica 5, A.R.G. Gantner Verlag K.G., Königstein, Germany

Metzeltin D, Lange-Bertalot H (2007) Tropical diatoms of South America II. Iconographia Diatomologica 18, A.R.G Gantner Verlag K.G., Königstein, Germany

Meyers PA, Teranes JL (2001) Sediment organic matter. In: Last WM, Smol JP (eds), Tracking Environmental Change Using Lake Sediments, Volume 2: Physical and Geochemical Methods. Kluwer, Dordrecht, pp 239-269

Michelutti N, Wolfe AP, Cooke CA, Hobbs WO, Vuille M, Smol JP (2015a) Climate change forces new ecological states in tropical Andean lakes. PLoS ONE 10: 1-10 doi:10.1371/journal.pone.0115338

Michelutti N, Lemmen, JL, Cooke, CA, Hobbs, WO, Wolfe, AP, Kurek, J, Smol, JP (2015b) Assessing the effects of climate and volcanism on diatom and chironomid assemblages in an Andean lake near Quito, Ecuador. Journal of Limnology doi:10.4081/jlimnol.2015.1323

Michelutti N, Lemmen JL, Cooke CA, Hobbs WO, Wolfe AP, Kurek J, Smol JP (2016) Assessing the effects of climate and volcanism on diatom and chironomid assemblages in an Andean lake near Quito, Ecuador. J Limnol 75: 275-286 doi: 10.4081/jlimnol.2015.1323

Morales EA, Vis ML, Fernández E, Kociolek JP (2007) Epilithic diatoms (Bacillariophyta) from cloud forest and alpine streams in Bolivia, South America II: A preliminary report on the diatoms from Sorata, Department of La Paz. Acta Nova 3: 680-696

Morales EA, Fernández E, Kociolek PJ (2009) Epilithic diatoms (Bacillariophyta) from cloud forest and alpine streams in Bolivia, South America 3: diatoms from Sehuencas, Carrasco National Park, Department of Cochabamba. Acta Bot Croat 68: 263-283

Morueta-Holme N, Engemann K, Sandoval-Acuña P, Jonas JD, Segnitz RM, Svenning J (2015) Strong upslope shifts in Chimborazo's vegetation over two centuries since Humboldt. PNAS 112: 12741-12745 doi: 10.1073/pnas.1509938112

Moscol-Olivera MC, Hooghiemstra H (2010) Three millennia upper forest line changes in northern Ecuador: pollen records and altitudinal vegetation distributions. Rev Palaeobot Palynol 163: 113-126 doi: 10.1016/j.revpalbo.2010.10.003

Mosquera PV, Hampel H, Vázquez RF, Alonso M, Catalan J (2017) Abundance and morphometry changes across the high-mountain lake-size gradient in the tropical Andes of southern Ecuador. Water Resour Res 53: 7269-7280 doi: 10.1002/2017WR020902

Niemann H, Matthias I, Michalzik B, Behling H (2013) Late Holocene human impact and environmental change inferred from multi-proxy lake sediment record in the Loja region, southeastern Ecuador. Quat Int 308-309: 253-264 doi: 10.1016/j.quaint.2013.03.017

Ochoa-Tocachi BF, Bardales JD, Antiporta J, Pérez K, Acosta L, Mao F, Zulkafli Z, Gil-Ríos J, Angulo O, Grainger S, Gammie G, De Biévre B, Buytaert W (2019) Potential contributions of pre-Inca infiltration infrastructure to Andean water security. Nat Sustain 2: 584-593 doi: 10.1038/s41893-019-0307-1

Pappas JL (2010) Phytoplankton assemblages, environmental influences and trophic status using canonical correspondence analysis, fuzzy relations, and linguistic translation. Ecol Inform 5: 79-88 doi: 10.1016/j.ecoinf.2009.08.005

Prado LF, Wainer I, Chiessi CM, Ledru MP, Turcq B (2013) A mid-Holocene climate reconstruction for eastern South America. Clim Past 9: 2117-2133 doi: 10.5194/cp-9-2117-2013,2013.

Rabatel A, Francou B, Soruco A, Gome J, Cáceres B, Ceballos JL, Basantes R, Vuille M, Sicart J-E, Huggel C, Scheel M, Lejeune Y, Arnaud Y, Collet M, Condom T, Consoli G, Favier V, Jomelli V, Galarraga R, Ginot P, Maisincho L, Mendoza J, Ménégoz M, Ramirez E, Ribstein P, Suarez W, Villacis M, Wagnon P (2013) Current state of glaciers in the tropical Andes: a multi-century perspective on glacier evolution and climate change. Cryosphere 7: 81-102 doi: 10.5194/tc-7-81-2013

Reimer PJ, Bard E, Bayliss A, Beck JW, Blackwell PG, Bronk Ramsay C, Buck CE, Cheng H, Edwards RL, Friedrich M, Grootes PM, Guilderson TP, Haflidason H, Hajdas I, Hatté C, Heaton TJ, Hoffman DL, Hogg AG, Hughen KA, Kaiser KF, Kromer B, Manning SW, Niu M, Reimer RW, Richards DA, Scott EM, Southon JR, Staff RA, Turney CSM, van der Plicht J (2013) IntCal13 and Marine13 radiocarbon age calibration curves 0-50,000 years cal BP. Radiocarbon 55: 1869-1887 doi: 10.3458/azu_js_rc.55.16947

Rühland KM, Paterson AM, Smol JP (2015) Lake diatom response to warming: reviewing the evidence. J Paleolimnol 54: 1-35 doi: 10.1007/s10933-015-9837-3

Rumrich U, Lange-Bertalot H, Rumrich M (2000) Diatoms of the Andes, from Venezuela to Patagonia/Tierra del Fuego, and two additional contributions. Iconographia diatomologica 9 A.R.G. Garner Verlag K.G., Königstein, Germany

Sarmiento F (2012) Contesting Páramo: Critical Biogeography of the Northern Andean Highlands. Kona Publishers, Charlotte, North Carolina, USA

Schneider T, Hampel H, Mosquera PV, Tylmann W, Grosjean M (2018) Paleo-ENSO revisited: Ecuadorian Lake Pallcacocha does not reveal a conclusive El Niño signal. Global Planet Change 168: 54-66 doi: 10.1016/j.gloplacha.2018.06.004

Schneider T, Bandow B, Bigalke M, Mestrot A, Hampel H, Mosquera PV, Fränkl L, Wienhues G, Vogel H, Tylmann W, Grosjean M (2021) 250-year records of mercury and trace element deposition in two lakes from Cajas National Park, SW Ecuadorian Andes. Environ Sci Pollut R doi: 10.1007/s11356-020-11437-0

Schnurrenberger D, Russell J, Kelts K (2003) Classification of lacustrine sediments based on sedimentary components. J of Paleolimnol 29: 141-154 doi: 10.1023/A:1023270324800

Servant-Vildary S (1986) Les diatomées actuelles des Andes de Bolivie (Taxonomie, écologie). Cahiers de Micropaléontologie 1:99-124

Sklenář P, Hedberg I, Cleef AM (2014) Island biogeography of tropical alpine floras. J Biogeog 41: 287-297 doi: 10.1111/jbi.12212

Stansell ND, Rodbell DT, Abbota MB, Mark BG (2013) Proglacial lake sediment records of Holocene climate change in the western Cordillera of Peru. Quat Sci Rev 70: 1-14 doi: 10.1016/j.quascirev.2013.03.003

Stone JR, Fritz SC (2004) Three-dimensional modeling of lacustrine diatom habitat areas: Improving paleolimnological interpretations of planktic:benthic ratios. Limnol Oceanog 49: 1540-1548 doi: 10.4319/lo.2004.49.5.1540

Turkia, J., Lepistö, L. (1999) Size variations in planktonic *Aulacoseira* Thwaites (Diatomae) in water and in sediment from Finnish lakes of varying trophic state. J Plankton Res 21: 757-770

Tylmann W (2014) Reply to the comment by F. Gharbi on "Multiple dating of varved sediments from Lake Lazduny, northern Poland: Toward an improved chronology for the last 150 years." Quat Geochronol 20: 111-113

Urrutia R, Araneda A, Cruces F, Torres L, Chirinos L, Treutler HC, Fagel N, Bertrand S, Alvial I, Barra R, Chapron E (2007) Changes in diatom, pollen, and chironomid assemblages in response to a recent volcanic event in Lake Galletué (Chilean Andes). Limnologica 37: 49-62

Velásquez-Ruiz CA, Hooghiemstra H (2013) Pollen-based 17-kyr forest dynamics and climate change from the Western Cordillera of Colombia; no-analogue associations and temporarily lost biomes. Rev Palaeobot Palynol 194: 38-49 doi: 10.1016/j.revpalbo.2013.03.001

Vélez MI, Wille M, Hooghiemstra H, Metcalfe S (2005) Integrated diatom-pollen based Holocene reconstruction of lake Las Margaritas, eastern savannas of Colombia. Holocene 15: 1184-1198 doi: 10.1191/0959683605hl890rp

Vélez MI, Hooghiemstra H, Metcalfe S, Wille M, Berrío JC (2006) Late Glacial and Holocene environmental and climatic changes from a limnological transect through

Colombia, northern South America. Palaeogeog Palaeoclimatol Palaeoecol 234: 81-96 doi: 10.1016.jpalaeo.2005.10.020

Villota A, Behling H, León-Yánez S (2017) Three millennia of vegetation and environmental dynamics in the Lagunas de Mojanda region, northern Ecuador. Acta Palaeobot 57: 407-421 doi: 10.1515/acpa-2017-0016

Vuille M, Bradley RS (2000) Mean annual temperature trends and their vertical structure in the tropical Andes. Geophys Res Letters 27: 3885-3888 doi: 10/1029/2000GL011871

Vuille M, Bradley RS, Werner M, Keimig F (2003) 20th century climate change in the tropical Andes: Observations and model results. Clim Change 59: 75-99 doi: 10.1023/A:1024406427519

Vuille M, Francou B, Wagnon P, Juen I, Kaser G, Mark BG, Bradley RS (2008) Climate change and tropical Andean glaciers: Past, present and future. Earth Sci Rev 89: 79-96 doi: 10.1016/j.earscirev.2008.04.002

Wanner H, Beer J, Butikofer J, Crowley TJ, Cubasch U, Fluckger J, Goosse H, Grosjean M, Joos F, Kaplan JO, Kuttel M, Muller SA, Prentice IC, Solomina O, Stocker TF, Tarasov P, Wagner M, Widmann M (2008) Mid- to Late Holocene climate change: an overview. Quat Sci Rev 27: 1791-1828 doi: 10.1016/j.quascirev.2008.06.013

Weide DM, Fritz SC, Hastorf CA, Bruno M, Baker PA, Guedron S, Salenbien W (2017) A ~6000-year diatom record of mid- to late-Holocene fluctuations in the level of Lago Wiñaymarca, Lake Titicaca, (Peru/Bolivia). Quaternary Res 88: 179-182 doi: 10.1017/qua.2017.49

Wolin, JA, Stone, JR (2010) Diatoms as indicators of water-level change in freshwater lakes. In: The Diatoms Applications to the Environmental and Earth Sciences, (eds) Stoermer, EF, Smol, JP. Cambridge University Press, 174-185

Wolfe AP, Kling HJ (2001) A consideration of some North American soft-water *Brachysira* taxa and description of *B. arctoborealis* sp. nov. In: Jahn R, Kociolek JP, Witkowski A, Compére P (eds), Lange-Bertalot-Festschrift: 243-264. Gantner Verlag, Ruggell

Tables

Table 1 Modern physico-chemical characteristics from Lagunas Fondococha and Piñan

Parameter	**Fondococha**	**Piñan**
Latitude (˚N)	-2.760	0.506
Longitude (˚E)	-79.236	-78.444
Elevation (m asl)	4130	3183
z_{max} (m)	9.8	32.14
Core H_2O Depth (m)	9.8	6
Core Length (cm)	105	70
Temperature (°C)	11.05	16.2
Secchi Depth (m)	2	3.5
pH	7.3	8.7
Conductivity (µS cm^{-1})	52.8	23.2
Ca (mg/L)	7.25	0.92
Mg (mg/L)	0.43	0.36
K (mg/L)	0.27	0.62
Na (mg/L)	0.8	1.08
Cl (mg/L)	0.13	0.08
SO_4 (mg/L)	0.42	0.54
TN (mg/L)	0.2	0.239

Figure Captions

Fig. 1 Digital elevation model (DEM) of the northern Andes and adjoining regions of South America, displaying site locations mentioned in the text. Black circles indicate lakes in this study, white circles indicate lake locations in the discussion, white squares are major cities, and the white star is the capital city

Fig. 2 Bathymetric maps of Fondococha (left), and Piñan (right). Coring locations are indicated by black squares.

Fig. 3 Relative abundance of the dominant diatom species in the **A**) Fondococha periphyton, **B**) Fondococha surface sediment, **C**) Piñan periphyton, and **D**) Piñan surface sediment. Ac.mac = *A. macrocephalum,* Ac.min = *A. minutissimum*, Au.alp = *A. alpigena,* Au.amb = *A. ambigua*, Au.d.s = *A. distans* var. *septentrionalis*, Au.gra = *A. granulata* var. *angustissima*, Au.sub = *A. subarctica*, Cv.pse = *C. pseudoscutiformis*, Na.rad = *N. radiosa*, Ni.cla =*N.* cf. *clandestina*, Ni.ob = *N.* cf. *oberheimiana*, Psa.gris = *P. grischunum*, and Stla.pin = *S. pinnata sensu lato*

Fig. 4 Stratigraphic diagram of diatom relative abundance of the two dominant planktic species, the tychoplankton, and benthon plotted against core depth (cm), and age (BC/AD) for Fondococha. Also included are the ratio of planktic to benthic diatoms (P:B Ratio), the rarefied species richness, the first two principal components axes (PC1, PC2), and the elemental concentration of Ti (cps). Diatom CONISS zones are described in the text. Orange bars indicate intervals of very low relative abundances of *A. distans*, low P:B ratios, and high rarefied species richness simultaneously

Fig. 5 Principal components analysis (PCA) biplots for the Fondococha (top) and Piñan (bottom) diatom data. CONISS clusters indicated by the 95% confidence ellipses

Fig. 6 Stratigraphic diagram of diatom relative abundance of notable species plotted against core depth (cm) and age (BC/AD) for Piñan. Also included are the ratio of planktic to benthic diatoms (P:B), the rarefied species richness, the carbon to nitrogen ratio (C/N), $\delta^{13}C_{org}$, and the first two principal components axes (PC1, PC2). Diatom CONISS zones are described in the text. Gray bars indicate tephras or periods of diatom absence in the short core

Fig. 1

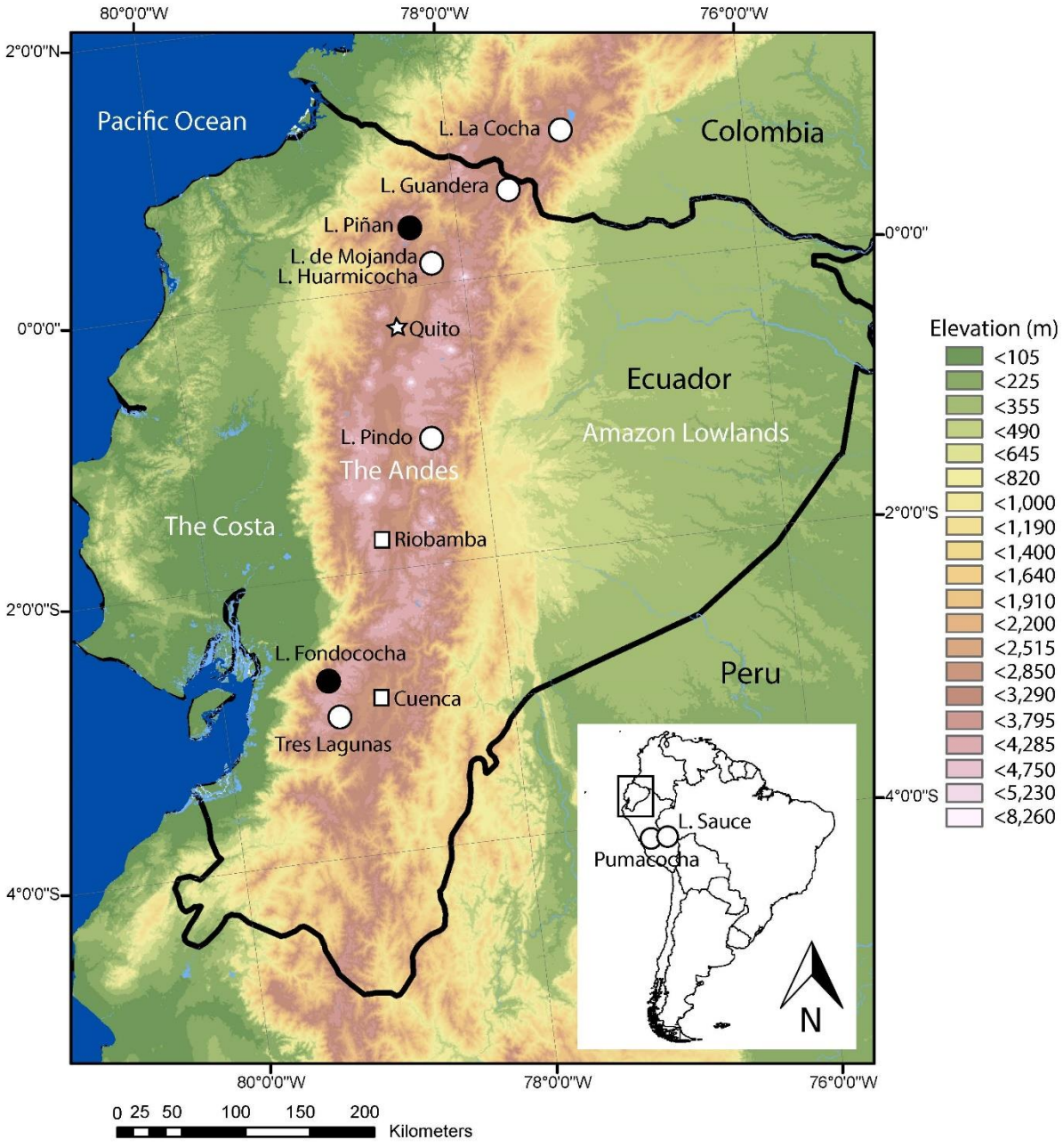
80°0'0"W
78°0'0"W
76°0'0"W
2°0'0"N
0°0'0"
2°0'0"S
4°0'0"S
Pacific Ocean
Colombia
L. La Cocha
L. Guandera
L. Piñan
L. de Mojanda
L. Huarmicocha
Quito
Ecuador
Amazon Lowlands
L. Pindo
The Andes
The Costa
Riobamba
L. Fondococha
Cuenca
Tres Lagunas
Peru
L. Sauce
Pumacocha
N
Elevation (m)
<105
<225
<355
<490
<645
<820
<1,000
<1,190
<1,400
<1,640
<1,910
<2,200
<2,515
<2,850
<3,290
<3,795
<4,285
<4,750
<5,230
<8,260
0 25 50 100 150 200
Kilometers

Figure 2

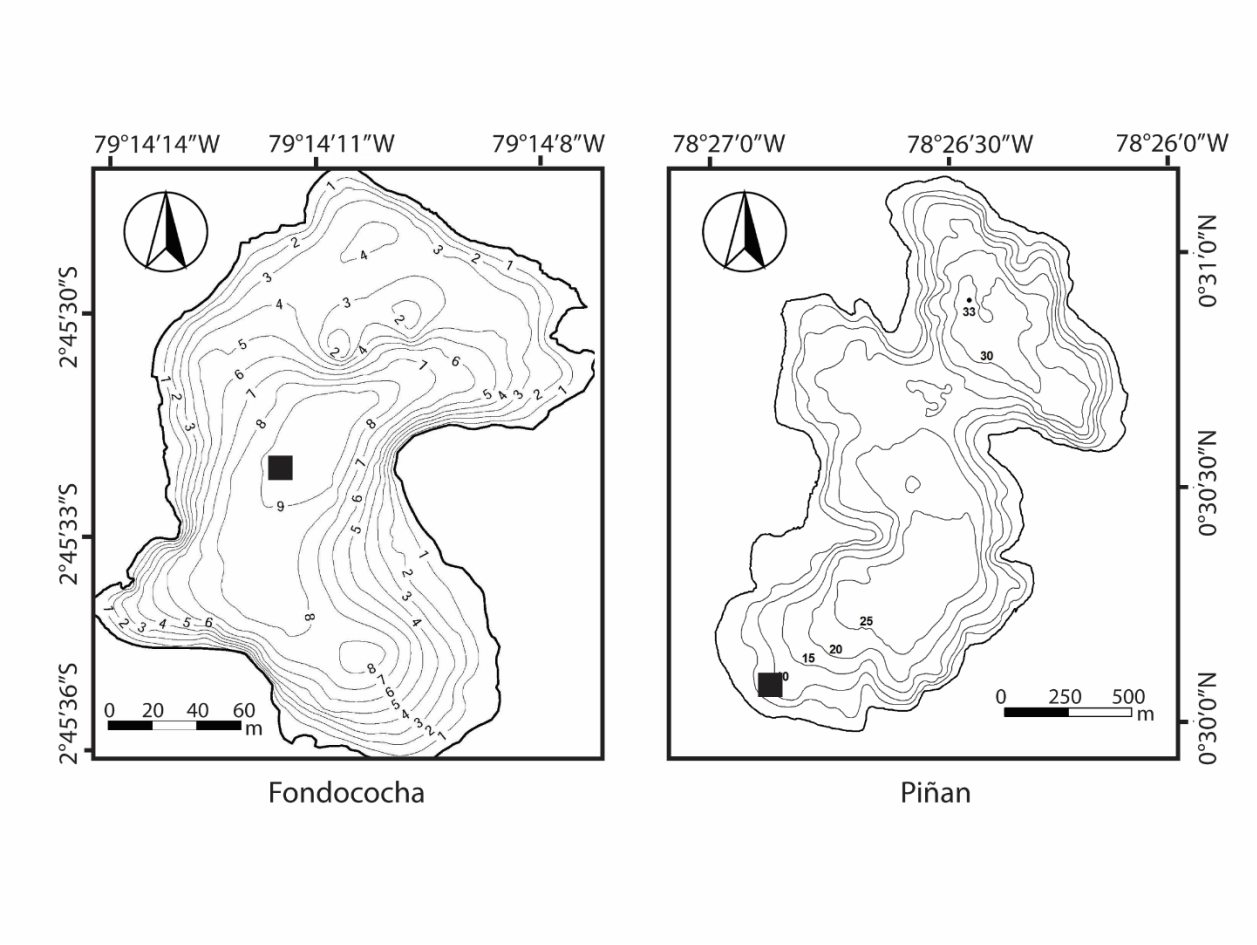
79°14′14″W
79°14′11″W
79°14′8″W
2°45′30″S
2°45′33″S
2°45′36″S
0 20 40 60 m
Fondococha
78°27′0″W
78°26′30″W
78°26′0″W
0°31′0″N
0°30′30″N
0°30′0″N
0 250 500 m
Piñan

Figure 3

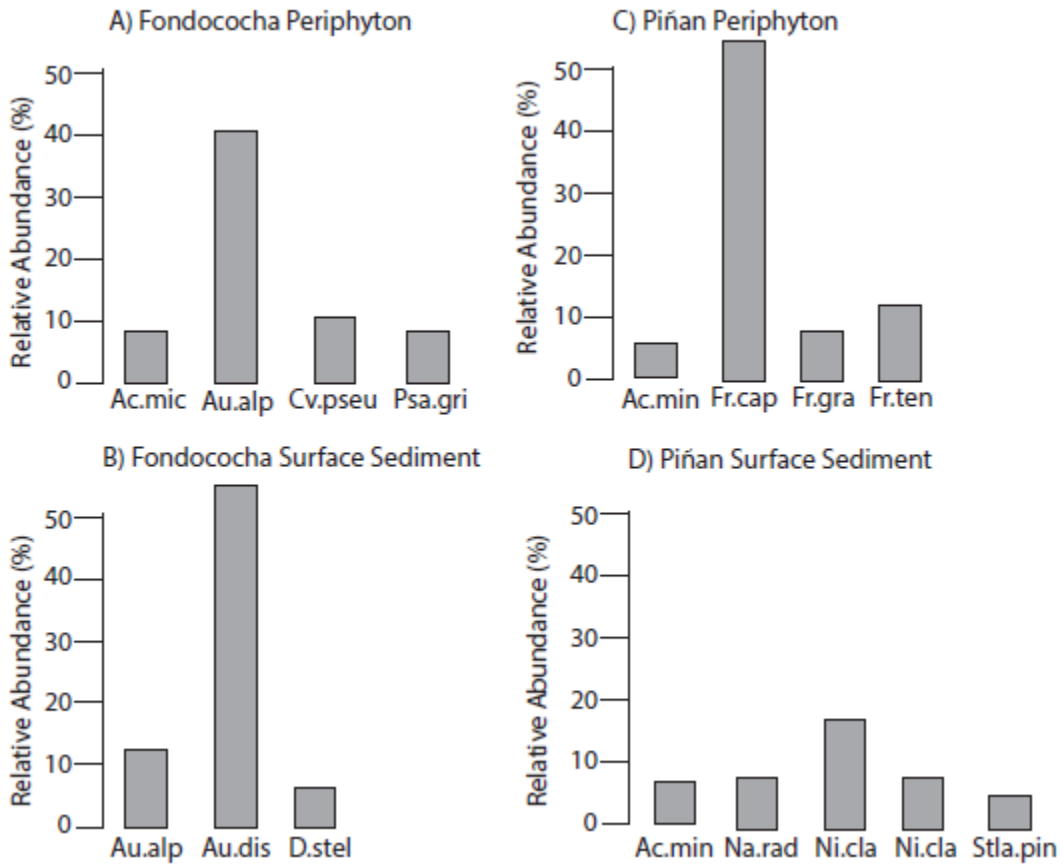
A) Fondococha Periphyton
Relative Abundance (%)
50
40
30
20
10
0
Ac.mic
Au.alp
Cv.pseu
Psa.gri
C) Piñan Periphyton
Relative Abundance (%)
50
40
30
20
10
0
Ac.min
Fr.cap
Fr.gra
Fr.ten
B) Fondococha Surface Sediment
Relative Abundance (%)
50
40
30
20
10
0
Au.alp
Au.dis
D.stel
D) Piñan Surface Sediment
Relative Abundance (%)
50
40
30
20
10
0
Ac.min
Na.rad
Ni.cla
Ni.cla
Stla.pin

Figure 4

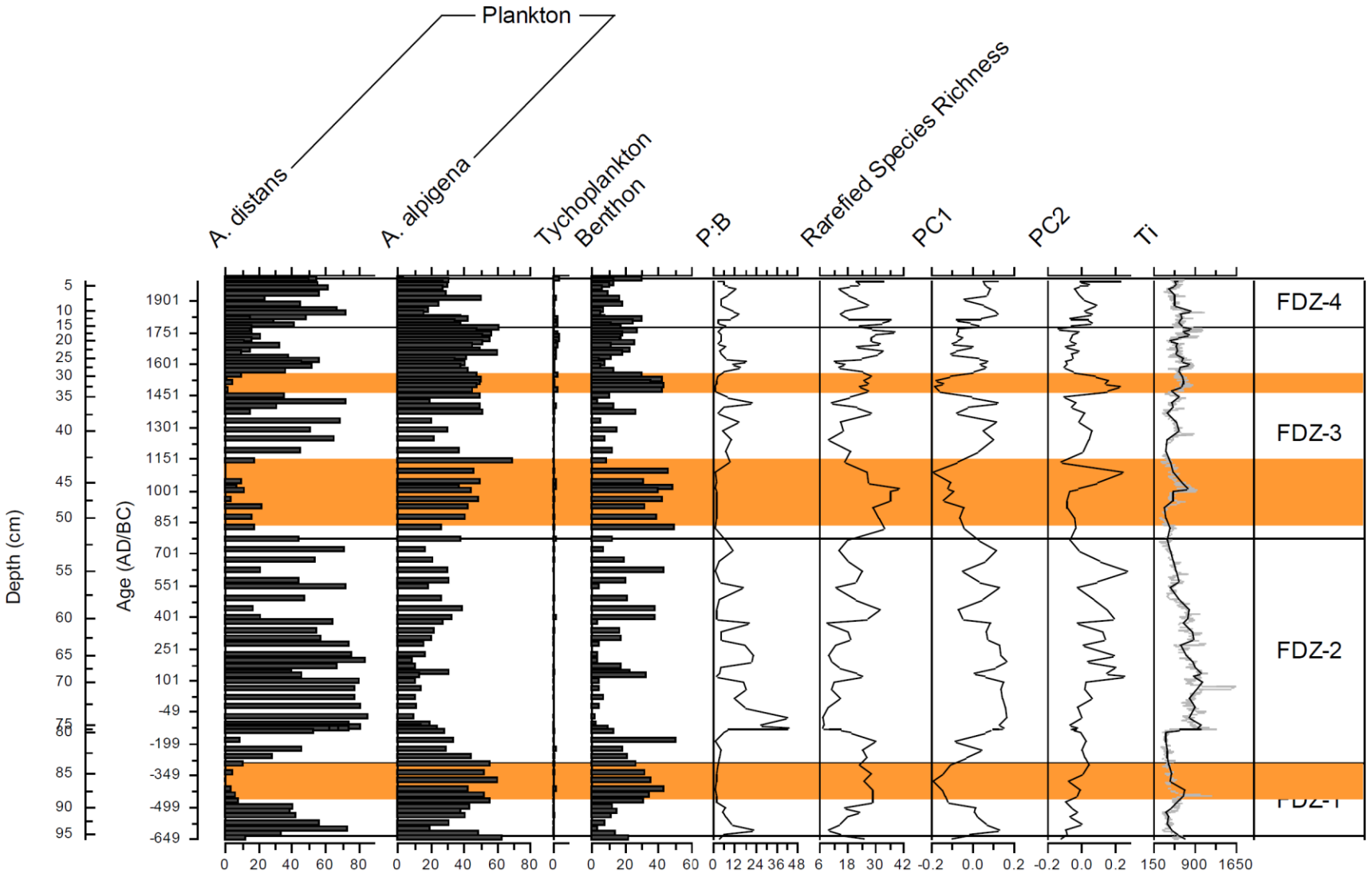
Plankton
A. distans
A. alpigena
Tychoplankton
Benthon
P:B
Rarefied Species Richness
PC1
PC2
Ti
Depth (cm)
Age (AD/BC)
FDZ-4
FDZ-3
FDZ-2
FDZ-1

Figure 5

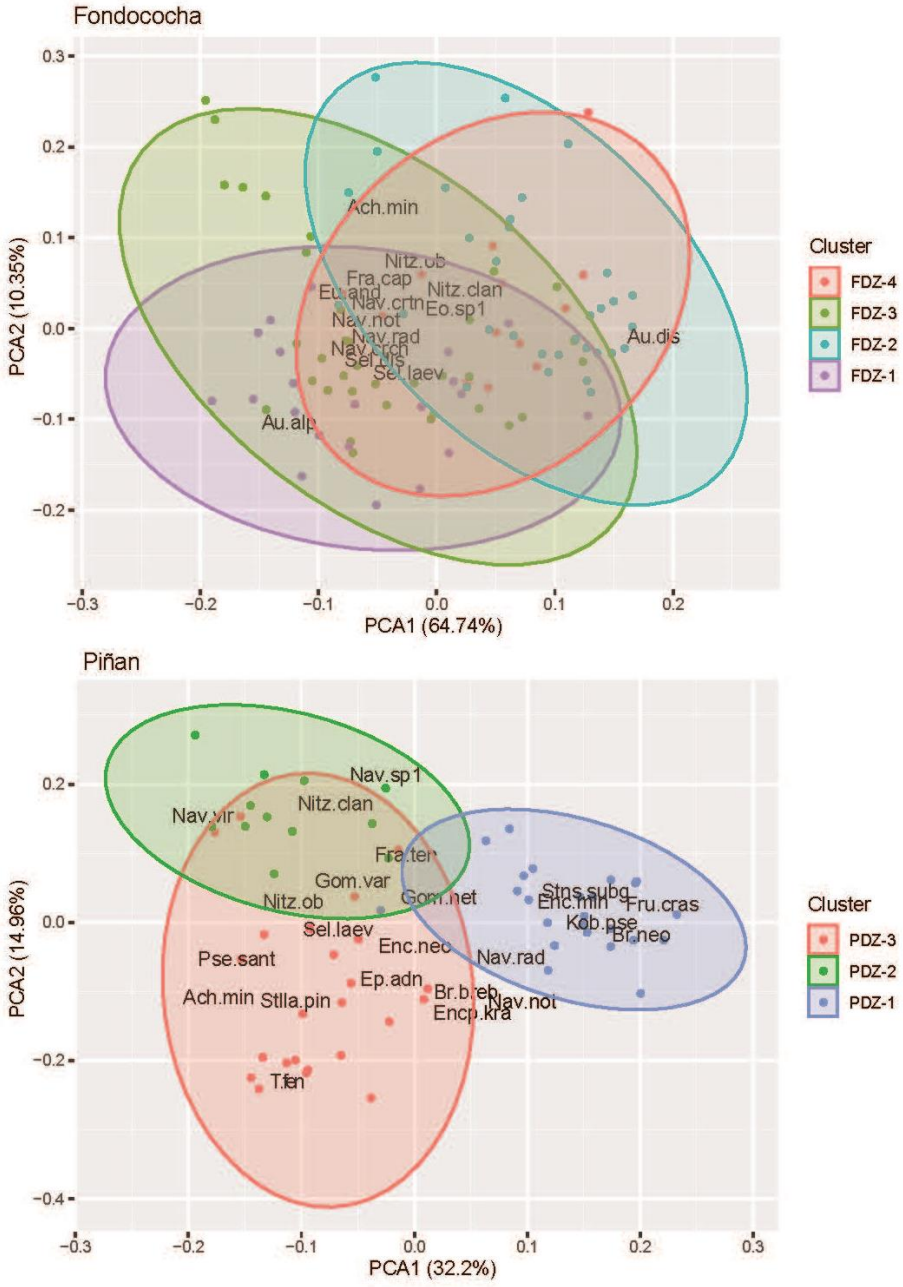
Fondococha
PCA2 (10.35%)
PCA1 (64.74%)
Ach.min
Fra.cap
Nav.crtn
Nav.not
Nav.rad
Sel.dis
Sel.laev
Eo.sp1
Au.dis
Au.alp
Cluster
FDZ-4
FDZ-3
FDZ-2
FDZ-1
Piñan
PCA2 (14.96%)
PCA1 (32.2%)
Nav.sp1
Nitz.clan
Gom.var
Nitz.ob
Sel.laev
Enc.neo
Pse.sant
Ach.min
Stlla.pin
Ep.adn
Nav.rad
Nav.not
Fru.cras
Br.neo
Cluster
PDZ-3
PDZ-2
PDZ-1

Figure 6

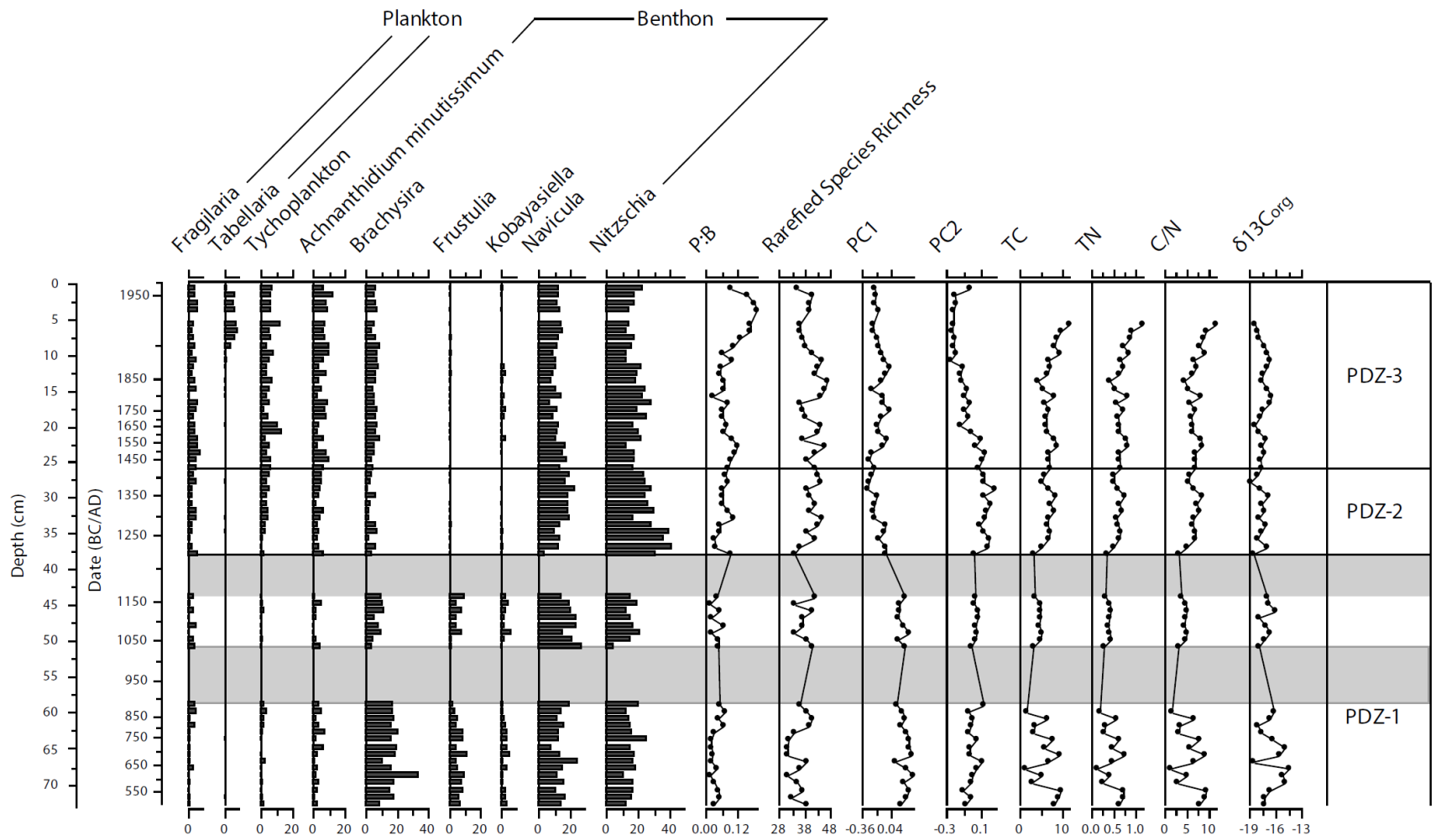
Plankton
Benthon
Fragilaria
Tabellaria
Tychoplankton
Achnanthidium minutissimum
Brachysira
Frustulia
Kobayasiella
Navicula
Nitzschia
P:B
Rarefied Species Richness
PC1
PC2
TC
TN
C/N
δ13Corg
Depth (cm)
Date (BC/AD)
PDZ-3
PDZ-2
PDZ-1